International Journal of Materials and Chemistry 2014, 4(3): 51-64
DOI: 10.5923/j.ijmc.20140403.02

Molecular Structure and Vibrational Analysis of 2-Amino- 5-(*m*-Nitrophenyl)-1,3,4-Thiadiazole by DFT Calculations

Mahesh Pal Singh Yadav, Anuj Kumar*

Department of Physics, Jaypee University of Engineering and Technology, Raghogarh, Guna, 473226, India

Abstract The 1,3,4-thiadiazole nucleus is one of the most important and well-known heterocyclic nuclei, which is a common and integral feature of a variety of natural products and medicinal agents. The role of thiadiazole and their derivatives has been very well established as pharmacologically significant scaffolds. Introduction of a nitro group into the benzene ring is of particular interest both for the elucidation of the influence of electron-withdrawing substituents on the reactivity of donor centers of heterocyclic compounds and for the subsequent synthesis of thiadiazole derivatives based on the reduced nitro group. The effect on delocalization of electron density (ED) and donor acceptor interaction due to change in substituents affects pharmacological activities significantly. In the present work, in an attempt to understand, the structure activity relation in an 1,3,4-thiadiazole we report optimized molecular structure confirmed by predictive vibrational spectra (IR/Raman spectra) and electronic behavior of one of the thiadiazole derivative 2-amino-5-(*m*-nitrophenyl)-1,3,4-thiadiazole. The calculations were made by density functional theory (DFT) using Becke's three-parameter hybrid functional (B3LYP) at various level of theory. The natural bond orbital analysis (NBO) has been performed in order to study the intramolecular bonding interactions among bonds and delocalization of unpaired electrons. These intramolecular charge transfer (n–σ*, n–π* and π-π*) can induce biological activities such as antimicrobials, anti-inflammatory, anti-fungal etc. in the molecule. Calculated band gap of 2.426 eV and global reactivity descriptors using HOMO-LUMO energies explain chemical and biological activity.

Keywords 1,3,4-Thiadiazole, Density functional theory, Structure activity relation, Charge transfer, IR/Raman spectra, HOMO-LUMO, Natural bond analysis (NBO)

1. Introduction

Heterocyclic compounds are ring compounds containing carbon and other element, the component being oxygen, nitrogen and sulphur. Thiadiazoles are heterocyclic compounds containing two nitrogen atoms and one sulfur atom as part of the aromatic five-membered ring. 1,3,4-thiadiazole are important because of their versatile biological actions[1]. There are number of thiadiazoles which contain the nitrogen in different positions such as 1,2,3-thiadiazole [2], 1,2,4-thiadiazole [3], 1,3,4-thiadiazole [4] and 1,2,5-thiadiazole [5] and their benzo derivatives [6] etc. 1,3,4-thiadiazole Derivatives shows a wide range of biological, pharmacological, and antileukemic activities [7-9]. Large number of such compounds have been synthesized and studies for their spectroscopic behavior and biological activity [3-6, 10].

* Corresponding author:
anuj.kumar@juet.ac.in (Anuj Kumar)
Published online at http://journal.sapub.org/ijmc

We have selected 2-amino-5-(m-nitrophenyl)-1,3,4 -thiadiazole, abbreviated as AMNT, one of the simplest 1,3,4-thiadiazole derivative for our study. To the best of our knowledge, despite of potential pharmacological applications, this molecule is not undergone any comprehensive stereoelectronic and spectroscopic studies. 2-amino-5-(m-nitrophenyl)-1,3,4- thiadiazole showed monoclinic packing having cell parameter a = 11.832 Å, b = 9.862 Å, c = 8.353 Å, V = 913.63 $Å^3$, d_{calcd} = 1.212 g cm^{-3} with space group P21/c [11]. Introduction of a nitro group into the benzene ring is of particular interest both for the elucidation of the influence of electron-withdrawing substituents on the reactivity of donor centers of heterocyclic compounds and for the subsequent synthesis of thiadiazole derivatives based on the reduced nitro group. Replacing the substituent in the phenyl group at position 3 of the 1,3,4-thiadiazole compounds with electron withdrawing groups, like halogens, nitriles, carbonyls etc. leads to affect biological activities [9].

In the present study, in an attempt to understand the structure property relation, the stereoelectronic interactions associated with the structural properties of 2-amino

-5-(*m*-nitrophenyl)-1,3,4-thiadiazole were investigated computationally using density functional theory (DFT) and ab initio methods. Therefore, we report optimized molecular structure confirmed by predictive vibrational spectra (FTIR/Raman) and physicochemical behavior for 2-amino-5-(*m*-nitrophenyl)-1,3,4-thiadiazole. In order to find conformational stability of the 2-amino-5-(m-nitrophenyl)-1,3,4-thiadiazole molecule, a potential energy scan is performed, and the corresponding relative energies were compared. The equilibrium geometry, harmonic vibrational wavenumbers, electrostatic potential surfaces, absolute Raman scattering activities and infrared absorption intensities have been calculated by DFT [12] with B3LYP functionals using various basis sets and HF/6-311G(d,p) with the help of Gaussian 09W package [13]. The calculated vibrational spectra were analyzed on the basis of the potential energy distribution (PED) of each vibrational mode which allowed us to obtain a quantitative as well as qualitative interpretation of the infrared and Raman spectra. To understand structure property relationship, HOMO-LUMO, electrostatic potential surface and natural bond orbitals have been obtained. Natural bond orbital analysis has been carried out to understand the nature of different interactions responsible for the electron delocalization and the intra-molecular charge transfer between the orbitals. These intra-molecular charge transfer (n–σ*, n–π* and π-π*) can induce biological activities such as antimicrobials, anti-inflammatory, anti-fungal, antibiotic, diuretic, antidepressant, anticancer, anticonvulsants, etc. in the molecule.

2. Computational Details

Computational aspects for geometry optimization and electronic structure of the stable conformers of the molecule have been done by density functional theory [12] by using the Gaussian 09W program package[13] employing different basis sets and Becke's three parameter (local, nonlocal, Hartree–Fock) hybrid exchange functionals with Lee–Yang–Parr correlation functionals (B3LYP) [14-16]. Infrared absorption intensities and Raman intensities have been calculated in the harmonic approximation with the help of same functional and basis sets as used for the optimized geometries, from the derivatives of the dipole moment and polarizability of each normal mode, respectively. The normal-mode analysis was used to calculate PED for each of the internal coordinates using no symmetry [17-18]. In order to prepare PED a complete set of 57 internal coordinates was defined using Pulay's recommendations [19, 20]. The vibrational assignments of the normal modes were proposed on the basis of the PED calculated using the program GAR2PED [21]. Calculated DFT vibrational wavenumbers are known to be higher than the experimental wavenumbers as the anharmonicity effects are neglected. Therefore, wavenumbers obtained by DFT were scaled down by the wavenumber linear scaling procedure (WLS) $\nu_{obs} = (1.0087–0.0000163\nu_{calc.})\ \nu_{calc.}\ cm^{-1}$ [22]. The WLS method using this relationship predicts vibrational wavenumbers with high accuracy and is applicable to a large number of compounds, except for those where the effect of dispersion forces is significant. All the calculated vibrational wavenumbers reported in this study are the scaled values. In order to investigate intra-molecular charge transfer interactions, rehybridization and delocalization of electron density within the molecule, the natural bonding orbitals (NBO) analysis has been performed. The main natural orbital interactions were analyzed on the basis of NBO calculations done at DFT/B3LYP level using Gaussian 09W package. In the NBO analysis [23, 24], the electronic wave functions are interpreted in terms of a set of occupied Lewis-type (bond or lone pair) and a set of unoccupied non-Lewis (antibond or Rydberg) localized NBO orbitals. Delocalization of electron density (ED) between these orbitals corresponds to a stabilizing donor–acceptor interaction. The second-order perturbation theory has been employed to evaluate the stabilization energies of all possible interactions between donor and acceptor orbitals in the NBO basis. The delocalization effects can be estimated from off-diagonal elements of the Fock matrix in the NBO basis.

3. Results and Discussion

3.1. Geometry Optimization

The theoretical structure of title molecule have been calculated by DFT using B3LYP functional having extended basis sets 6-311++G(d,p), 6-311+G(d,p), 6-311G(d,p) and HF/6-311G(d,p) with the help of Gaussian 09W package and geometry obtained from B3LYP/6-311++G(d,p) is shown in Fig.1.

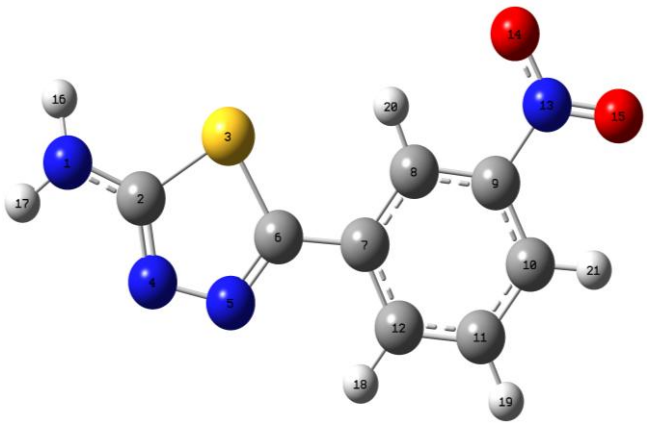

Figure 1. Optimized structure of AMNT at the B3LYP/6-311++G(d;p) level of theory

Table 1. Optimized geometrical parameters of AMNT by DFT in comparison with XRD data

Geometrical parameters	Experimental (XRD)	Optimized				Geometrical parameters	Experimental (XRD)	Optimized			
		B3LYP/ 6-311++G(d,p)*	B3LYP/ 6-311+G(d,p)	B3LYP/ 6-311G(d,p)	HF/ 6-311G(d,p)			B3LYP/ 6-311++G(d,p)*	B3LYP/ 6-311+G(d,p)	B3LYP/ 6-311G(d,p)	HF/ 6-311G(d,p)
C2-N1	1.402	1.367	1.367	1.366	1.367	C12-C7-C6	130.66	119.273	119.283	119.207	119.166
S3-C2	1.509	1.757	1.757	1.759	1.739	N13-C9-C8	111.63	118.483	118.487	118.497	118.518
N4-C2	1.352	1.305	1.305	1.305	1.272	O14-N13-C9	114.55	117.667	117.672	117.593	117.548
N5-N4	1.379	1.358	1.358	1.357	1.359	O15-N13-C9	112.06	117.620	117.620	117.534	117.525
C6-S3	1.869	1.775	1.775	1.776	1.753	H16-N1-C2	128.44	118.349	118.381	118.014	116.333
C7-C6	1.414	1.466	1.466	1.466	1.477	H17-N1-C2	118.18	114.179	114.210	113.554	112.687
C8-C7	1.125	1.397	1.397	1.397	1.383	H18-C12-C7	118.04	118.597	118.599	118.443	118.817
C9-C8	1.341	1.389	1.389	1.388	1.382	H19-C11-C12	135.51	119.698	119.695	119.699	119.856
C10-C9	1.34	1.389	1.389	1.388	1.377	H20-C8-C7	116.67	122.132	122.137	122.257	122.116
C11-C10	1.12	1.393	1.393	1.393	1.385	H21-C10-C11	115.73	122.116	122.114	122.314	121.703
C12-C7	1.362	1.406	1.406	1.406	1.394	N4-C2-N1-S3	178.65	176.118	176.124	176.030	176.450
N13-C9	1.187	1.481	1.481	1.481	1.464	N5-N4-C2-N1	-178.94	-176.324	-176.321	-176.215	-176.599
O14-N13	1.188	1.224	1.224	1.223	1.186	C6-S3-C2-N1	178.72	176.691	176.684	176.630	177.059
O15-N13	1.174	1.223	1.223	1.222	1.185	C7-C6-S3-C2	179.18	179.238	179.260	179.256	179.439
H16-N1	0.907	1.007	1.007	1.007	0.995	C8-C7-C6-S3	39.73	-0.1355	-0.260	-0.304	-1.627
H17-N1	0.907	1.010	1.010	1.010	0.997	C9-C8-C7-C6	-178.59	-179.960	-179.963	-179.971	-179.927
H18-C12	0.814	1.082	1.082	1.082	1.072	C10-C9-C8-C7	1.87	-0.064	-0.064	-0.056	-0.023
H19-C11	1.005	1.083	1.083	1.083	1.074	C11-C10-C9-C8	-3.98	0.035	0.037	0.027	0.026
H20-C8	0.928	1.081	1.081	1.081	1.071	C12-C7-C6-N5	37.92	-0.386	-0.513	-0.470	-1.484
H21-C10	0.877	1.080	1.080	1.080	1.071	N13-C9-C8-C7	-179.59	179.942	179.943	179.947	179.968
S3-C2-N1	118.39	122.493	122.491	122.445	121.852	O14-N13-C9-C8	10.75	-0.179	-0.161	-0.146	-0.155
N4-C2-N1	133.67	123.326	123.324	123.282	123.969	O15-N13-C9-C10	10.27	-0.154	-0.137	-0.123	-0.150
N5-N4-C2	122.48	112.674	112.669	112.623	112.642	H16-N1-C2-S3	12.1	30.604	30.463	32.844	37.998
C6-S3-C2	89.47	85.833	85.828	85.679	85.815	H17-N1-C2-N4	0.59	-12.990	-12.980	-12.433	-11.988
C7-C6-S3	129.12	123.594	123.601	123.540	123.902	H18-C12-C7-C6	-0.93	0.002	0.010	-0.004	-0.071
C8-C7-C6	114.39	121.761	121.753	121.828	121.541	H19-C11-C12-C7	178.71	179.969	179.975	179.969	-179.985
C9-C8-C7	111.91	119.144	119.148	119.148	119.006	H20-C8-C7-C6	0.8	0.036	0.027	0.036	0.057
C10-C9-C8	133.7	122.530	122.529	122.526	122.449	H21-C10-C11-C12	-172.23	-179.982	-179.992	-179.991	179.957
C11-C10-C9	113.71	118.011	118.009	118.042	118.163						

Geometry of $C_8H_6N_4O_2S$ (AMNT) was optimized without any constraint to the potential energy surface using given X-ray diffraction data as initial point [11]. All the optimized bond lengths and bond angles of the calculated $C_8H_6N_4O_2S$ molecule are tabulated in Table-1 along with the reported molecular parameters [11]. The title compound contains phenyl, amino, nitro and thiadiazole moieties. The five-membered thiadiazole ring is essentially planar. The dihedral angles between the phenyl and the thiadiazole ring is calculated at -0.135 °, but experimental data shows a twist of 39.73 °. This may be attributed to intermolecular interaction in the crystal packing. Only two bond distances in the thiadiazole ring show a double bond character C6=N5, C2=N4 with bond lengths 1.297 Å, 1.305 Å respectively and bonds S3-C6, S3–C2 with bond lengths 1.775 Å, 1.757 Å show the values of a single bond character. The S–C bond distances are found in good agreement with the accepted value for an S–C(sp2) single bond of bond length 1.76 Å [25]. In general, the calculated structural parameters match well with experimental data with few exceptions. The difference found in calculated values (in gas phase) from the experimental values may be due to the solid state intermolecular interactions related to crystal packing effects. It is worth noting that the C9–N13 bond distance value of 1.481 Å falls into the C=N double bond distance region and is shorter than the C=N double bond distance found in a related thiadiazole ring structure [26]. The bond C2-N1 shows the partial double bond character with bond length 1.367 Å.

3.2. Potential Energy Scan Studies

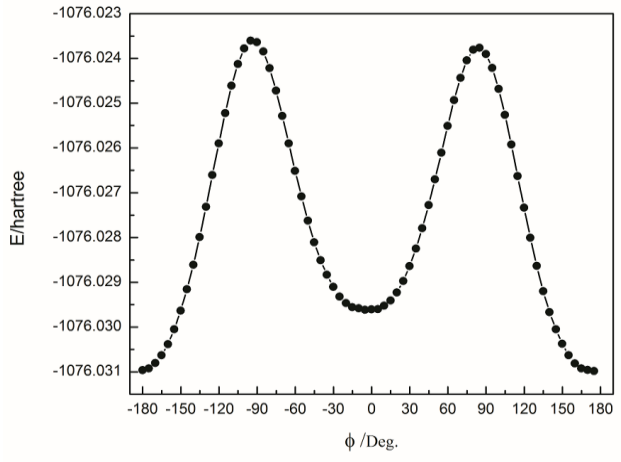

Figure 2. Potential energy scan of AMNT about dihedral angle (C12–C7–C6–S3) at B3LYP/6-311++g(d,p) level of theory

In order to investigate all possible conformations of 2-amino-5-(m-nitrophenyl)-1,3,4-thiadiazole, a detailed potential energy scan was performed for the dihedral angle ϕ(C12–C7–C6–S3) at B3LYP/6-311++g(d,p) level of theory with constraint nosymmetry. The scan studies was obtained by minimizing the potential energy in all geometrical parameters by varying the torsion angles at a step of 5 ° in the range of 0–360 ° rotation around the bond. The variations of the potential energy change from its equilibrium with the torsional perturbation are presented in Fig. 2. The PES scan revealed that the 2-amino-5-(m-nitrophenyl)-1,3,4 -thiadiazole molecule may have less stable conformer at torsion angle (C12–C7–C6–S3) equal to -5.23709 ° having energy -1076.029 Hartree (-2825114.354 kJ/mol). The most stable equilibrium state belongs to (C12–C7–C6–S3) =179.862 ° and potential energy equal to -1076.309 Hartree (-2825851.595 kJ/mol).

3.3. Natural Bond Orbital Analysis

NBO analysis is an efficient method for study of the intramolecular and intermolecular bonding and interactions among bonds. This analysis also provides the study of filled NBOs (donors) and empty NBOs (acceptors) and their interactions with the stabilization energy $E^{(2)}$ resulting from the second-order perturbation theory. The larger the $E^{(2)}$ value, the more intensive is the interaction between electron donors and acceptors, i.e. the more electron donating tendency from electron donors to acceptors and the greater the extent of conjugation of the whole system. This interaction results a loss of occupancy from the concentration of electron NBO of the idealized Lewis (bond or lone pair) structure into an empty (anti-bond or Rydberg) non-Lewis orbital. For each donor (i) and acceptor (j), the stabilization energy $E^{(2)}$ associated with the delocalization i – j is estimated as [23, 27, 17]:

$$E^{(2)} = -n_\sigma[\langle\sigma|F|\sigma\rangle^2/\varepsilon_{\sigma^*} - \varepsilon_\sigma] = -n_\sigma\left[\frac{F_{ij}^2}{\Delta E}\right]; \qquad (1)$$

Where $(\langle\sigma|F|\sigma\rangle^2)$ is the Fock matrix element which corresponds to i and j NBO orbitals. n_σ is the population of the donor σ orbital, ε_{σ^*} and ε_σ are the energies of σ* and σ NBOs. NBO calculations were performed using the NBO 5.9 program as implemented in the Gaussian 09 package at the DFT/B3LYP/6-311++G(d,p) level of the theory. The second-order perturbation theory analysis of Fock matrix in NBO basis of AMNT molecule display strong intra-molecular conjugative and hyperconjugative interactions and demystify the rehybridization and delocalization of electron density within the molecule. Some important interactions between Lewis and non-Lewis orbitals along with their interacting stabilization energies are shown in Table-2.

The Fock matrix analysis shows strong intra-molecular hyperconjugative interactions of π electrons between π bond orbitals and anti bonding orbitals. These interactions are established by the orbital overlapping between π(C–C or C-N) and π*(C–C or C-N) bond orbitals resulting ICT (Intramolecular charge transfer) causing stabilization of the system.

The electron density (ED) at the six conjugated π bonds (1.6–1.7e) and π* antibonds (0.1–0.4 e) of the phenyl ring clearly shows strong delocalization leading to stabilization of energy in the range of 12–23 kcal/mol. These results are consistent with as reported by C. James et al. [18]. The important interaction (n–π) energies associated with the

resonance in the molecule are electron donation from the LP(1) of atom N1, LP(2) of atom S3 (electron donating groups) to the anti-bonding acceptors π*(C2-N4) and π*(C2-N4) ,π*(N5-C6) of thiadiazole ring which correspond to the stabilization energies 38.22 and 27.80, 24.16 kcal/mol respectively. Similar interaction is observed from LP(3) of atom O14 to the anti-bonding acceptor π*(N13-O15) of nitro group having stabilization energy equal to 12.90 kcal/mol. These π*(C2-N4) and π*(N5-C6) antibonding orbitals of the thiadiazole ring further show hyperconjugation with π*(N5-C6) and π*(C7-C8) of phenyl ring respectively. This shows the intramolecular charge transfer from thiadiazole ring to phenyl ring with enormous amount of stabilization energies 173.73 and 101.66 kcal/mol respectively. A strong intramolecular interaction of π electrons occurs from π(C7-C8) and π(C11-C12) bonds to the π*(C9–C10) antibond corresponding to the stabilization energies 20.36 and 23.43 kcal/mol respectively. This enhanced π*(C9–C10) NBO further hyperconjugates with π*(C11–C12) correspond the high stabilization energy 223.26 kcal/mol.

The hyperconjugative interaction of σ(N1–H17) and conjugative interaction of σ(S3–C6) distribute over σ*(C2–S3) and (N1–C2) leads to the stabilization energies 6.51 and 5.53 kcal/mol respectively. The hyperconjugative interaction (n–σ*) between the electron-donating nitrogen atoms n1(N4) and n1(N5) of the thiadiazole ring and antibonding orbitals σ*(C2–S3), (N5-C6) and σ*(C2-N4), (S3–C6) leads to the stabilization energies 15.21,5.53 and 5.35,16.31 kcal/mol respectively. The charge transfer from lone pairs of n2(O14) and n2(O15) to antibonding orbitals σ*(C9–N13), (N13-O15) and σ*(C9–N13), (N13-O14) correspond to the stabilization energies 12.37, 18.95 and 12.47, 19.03 kcal/mol due to small energy difference between donor and acceptor respectively. These intramolecular charge transfer (n–σ*, n–π* and π-π*) may induced biological activities such as antimicrobials, anti-inflammatory, anti-fungal, antibiotic, diuretic, antidepressant, anticancer, anticonvulsants, etc. in the title molecule.

Table 2. Second-order perturbation theory analysis of Fock matrix in NBO basis

Donor NBO(i)	ED(i)/e	Acceptor NBO(j)	ED(j)/e	E(2)kcal/mol	E(j)-E(i)a.u.	F(i,j)a.u.
σ N1 - H17	1.980	σ* C2 - S3	0.082	6.51	0.84	0.067
π C2 - N4	1.874	π* N5 - C6	0.332	14.32	0.33	0.065
σ S3 - C6	1.976	σ* N1 - C2	0.024	5.53	1.10	0.070
π N5 - C6	1.897	π* C2 - N4	0.390	9.57	0.32	0.053
π N5 - C6	1.897	π* C7 - C8	0.352	9.65	0.35	0.056
π C7 - C8	1.632	π* N5 - C6	0.332	19.37	0.27	0.065
π C7 - C8	1.632	π* C9 - C10	0.375	20.36	0.28	0.067
π C7 - C8	1.632	π* C11 - C12	0.279	19.17	0.29	0.068
π C9 - C10	1.647	π* C7 - C8	0.352	21.71	0.29	0.071
π C9 - C10	1.647	π* C11 - C12	0.279	15.99	0.30	0.063
π C9 - C10	1.647	π* N13 - O15	0.618	12.87	1.77	0.145
π C11 - C12	1.640	π* C7 - C8	0.352	19.17	0.28	0.065
π C11 - C12	1.640	π* C9 - C10	0.375	23.43	0.27	0.072
π N13 - O15	1.986	n3 O14	1.448	12.47	0.18	0.079
n1 N1	1.803	π* C2 - N4	0.390	38.22	0.30	0.100
n2 S3	1.668	π* C2 - N4	0.390	27.80	0.25	0.076
n2 S3	1.668	π* N5 - C6	0.332	24.16	0.26	0.071
n1 N4	1.898	σ* C2 - S3	0.082	15.21	0.56	0.082
n1 N4	1.898	σ* N5 - C6	0.026	5.53	0.95	0.066
n1 N5	1.893	σ* C2 - N4	0.031	5.36	0.93	0.064
n1 N5	1.893	σ* S3 - C6	0.082	16.31	0.55	0.085
n2 O14	1.898	σ* C9 - N13	0.106	12.37	0.56	0.074
n2 O14	1.898	σ* N13 - O15	0.054	18.95	0.73	0.106
n3 O14	1.448	π* N13 - O15	0.618	12.90	1.77	0.137
n2 O15	1.898	σ* C9 - N13	0.106	12.47	0.56	0.075
n2 O15	1.898	σ* N13 - O14	0.054	19.03	0.73	0.106
π* C2 - N4	0.390	π* N5 - C6	0.332	173.73	0.01	0.064
π* N5 - C6	0.332	π* C7 - C8	0.352	101.66	0.02	0.067
π* C9 - C10	0.375	π* C11 - C12	0.279	233.26	0.01	0.083

3.4. Molecular Electrostatic Potential

Various weak interactions in 2-amino-5- (*m*-nitrophenyl)-1,3,4-thiadiazole molecule, such as C–H…π, π–π and weak hydrogen-bonding interactions have very important significance in determining stability of the molecule. The presence of amino and nitro group leads to the electronic coupling between ring electrons and nitrogen lone pair electrons which provides stabilization to the molecular structure and enhance its antilukemic properties. Hence it is important to study the electrostatic potential distribution in the molecule. The molecular electrostatic potential (MEP) is a property that the electrons and nuclei of a molecule create at each point r in the surrounding space [28]. Electrostatic potential provides very useful information to explain hydrogen bonding, reactivity and structure–activity relationship of molecules and correlates with dipole moment, electronegativity, partial charges and site of chemical reactivity of the molecule. It gives a visualization to understand the relative polarity of a molecule. The regions with negative MEP, correspond to the areas of high electron density representing a strong attraction between the proton and the points, on the molecular surface have the brightest red color. The positive valued regions, areas of lowest electron density, have deep blue to indigo color indicating the regions of maximum repulsion. The electron density isosurface onto which the electrostatic potential surface has been mapped is shown in Fig. 3 for 2-amino-5-(*m*-nitrophenyl)-1,3,4-thiadiazole. The different values of the electrostatic potential at the surface are represented by different colors; yellow represents regions of most negative electrostatic potential, blue represents regions of most positive electrostatic potential over the amino group and green represents regions of zero potential. From Fig. 3, it is visible that the region of the most negative electrostatic potential is spread over the O14, O15 atom of NO_2 group and N4, N5 of the thiadiazole ring. This indicates the delocalization of π electrons over the nitro group and thiadiazole ring. This also reveals extended conjugation of the phenyl rings with the nitro group.

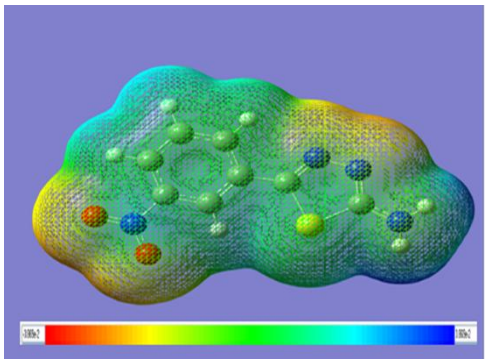

Figure 3. Molecular electrostatic potential mapped on the isodensity surface for AMNT calculated at the B3LYP/6-311++G(d;p) level of theory

3.5. HOMO-LUMO Analysis

The highest occupied molecular orbital (HOMO) and lowest unoccupied molecular orbital (LUMO) are the main orbitals that plays an important role in chemical stability [29]. The HOMO exhibits the ability to donate an electron and LUMO as an electron acceptor serves the ability to obtain an electron. The HOMO and LUMO energy calculated by B3LYP/6-311++G (d,p) level of theory show the energy gap which reflects the chemical activity of the molecule.

HOMO energy (B3LYP) = −782.609 kJ/mol

LUMO energy (B3LYP) = −548.520 kJ/mol

HOMO − LUMO energy gap (B3LYP) = 234.089 kJ/mol

The HOMO is positioned over the thiadiazole ring and amino group, the HOMO→LUMO transition implies an electron density transfer to Phenyl ring and nitro group from thiadiazole ring and amino group. This ICT between thiadiazole ring and Phenyl ring is responsible for existing biological activities. The atomic orbital compositions of the frontier molecular orbital are shown in Fig. 4.

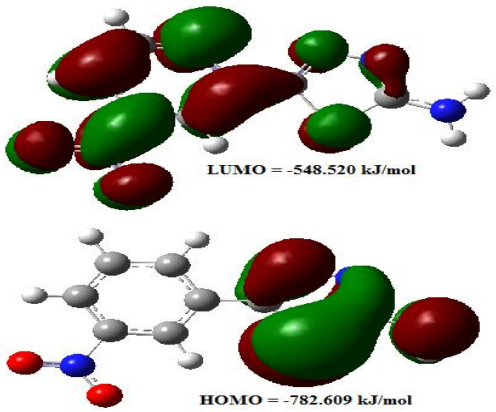

Figure 4. The molecular orbitals of AMNT at B3LYP/6-311++ G(d;p) level

On the basis of HOMO-LUMO energies global reactivity descriptors, such as the energies of frontier molecular orbitals (ε_{HOMO}, ε_{LUMO}), energy band gap ($\varepsilon_{HOMO} - \varepsilon_{LUMO}$), electronegativity (χ), chemical potential (μ), global hardness (η), global softness (S) and global electrophilicity index (ω), which describe the electrophilic behaviour [30-34], have been calculated for AMNT using Eqs. (2)–(6):

$$\chi = -\frac{1}{2}(\varepsilon_{LUMO} + \varepsilon_{HOMO}) = 665.564\ \text{kJ/mol} \quad (2)$$

$$\mu = -\chi = \frac{1}{2}(\varepsilon_{LUMO} + \varepsilon_{HOMO}) = -665.564\ \text{kJ/mol} \quad (3)$$

$$\eta = \frac{1}{2}(\varepsilon_{LUMO} - \varepsilon_{HOMO}) = 117.045\ \text{kJ/mol} \quad (4)$$

$$S = \frac{1}{2\eta} = 0.004\ \left(\frac{\text{kJ}}{\text{mol}}\right)^{-1} \quad (5)$$

$$\omega = \frac{\mu^2}{2\eta} = 1892.330\ \text{kJ/mol} \quad (6)$$

Electrophilic charge transfer (ECT) [30] is defined as the difference between the ΔN_{max} values of interacting molecules. For two molecules I and II approaching each other (i) if ECT > 0, charge flows from II to I and (ii) if ECT < 0, charge flows from I to II. ECT is calculated using Eq. (7):

$$ECT = (\Delta N_{max})_I - (\Delta N_{max})_{II} \quad (7)$$

where $(\Delta N_{max})_I = -\mu_I/\eta_I$ and $(\Delta N_{max})_{II} = -\mu_{II}/\eta_{II}$.

3.6. Vibrational Spectral Analysis

The vibrational spectra of 2-amino-5-(*m*-nitrophenyl) -1,3,4-thiadiazole molecule have been calculated by DFT with B3LYP functional having extended basis set 6-311G(d,p), 6-311+G(d,p), 6-311++G(d,p) and by HF with basis set 6-311++G(d,p) using Gaussian 09W package. Due to exclusion of anharmonicity, the calculated wave numbers are higher and therefore, scaled down by the wave number linear scaling procedure (WLS) [ν_{obs}/ν_{cal} = (1.0087 – 0.0000163 *ν_{cal}) cm^{-1}] given by Yoshida et al. [22]. This molecule has 21 atoms, which gives 57 (3n-6) normal modes. AMNT has phenyl and thiadiazole rings with different functional groups namely nitro and amino respectively. Vibrational mode assignments have been made on the basis of relative intensities, line shape and potential energy distribution obtained from normal coordinate analysis. All the 57 fundamental vibrations of the free molecule are both IR and Raman active. The calculated vibrational wave-numbers and their PED for each normal mode are presented in Table 3. The calculated (scaled) infrared absorbance and Raman spectra are shown in Fig. 5 and Fig. 6, respectively.

In order to make better understanding, the vibrational assignments have been studied separately for all groups and rings. We have discussed here only the dominant contributions to the total potential energy of normal modes of vibration out of several internal coordinates that may be present in the PED as shown in Table-3.

AMNT consist a thiadiazole ring (ring-1) having amino group attached at position 2. Ring-1 has two CS stretching vibrations which are calculated at 653 and 665 cm^{-1}. These modes have prominent contribution (10-60%) from CS stretch along with other vibrations of the ring-1and amino group. Two C-N antisymmetric and symmetric stretching vibrations are calculated at frequencies 1497 and 1507 cm^{-1} and are reported at 1517 and 1619 cm^{-1} [11] and for AMNO [35] it is reported at 1630 cm^{-1}. One prominent N-N stretching(49%) vibration is calculated at 1154 cm^{-1}, this mode is reported to be observed at 995 cm^{-1} [11]. These vibrations also have the contribution from other modes of ring-2 and amino group. The in-plane bending of ring-1 calculated at 440 cm^{-1} and out-of-plane bending of ring-1 occurs at 607 cm^{-1} having contribution from ring-2 deformation and other vibrations of amino group in the frequency range 85-740 cm^{-1}.

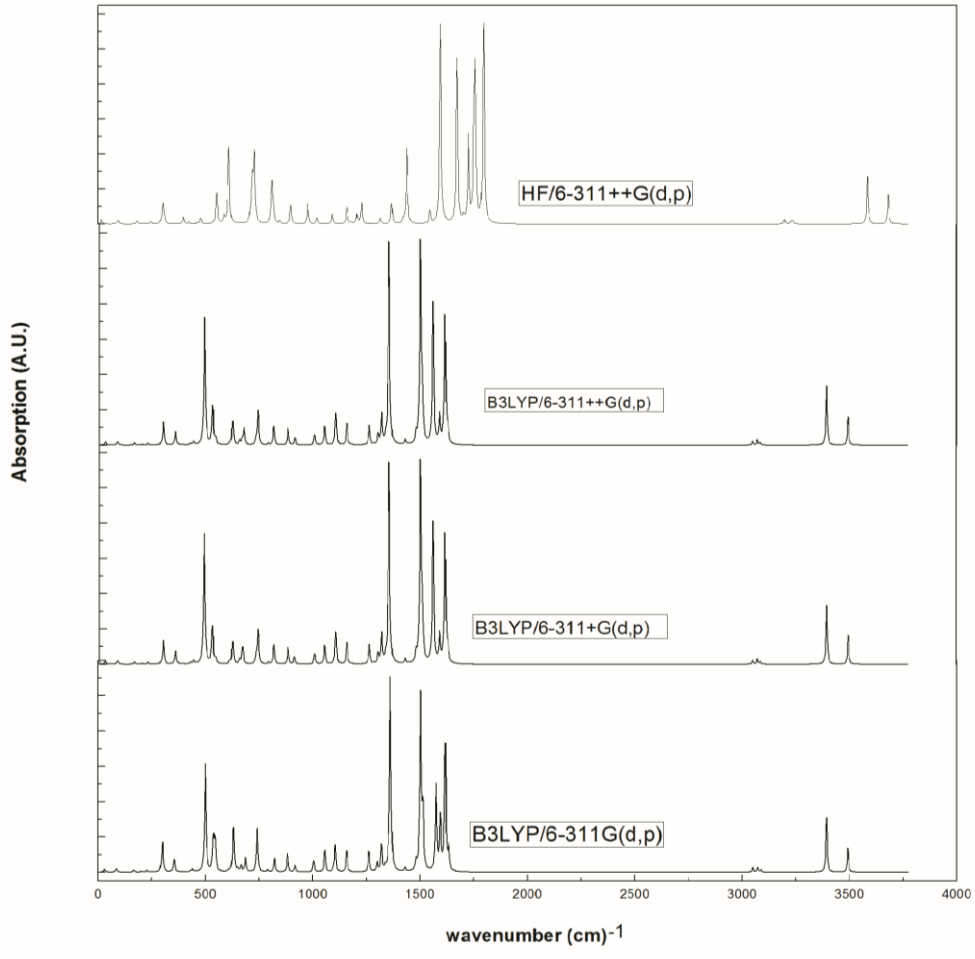

Figure 5. Calculated infrared spectra of AMNT at various level of theory

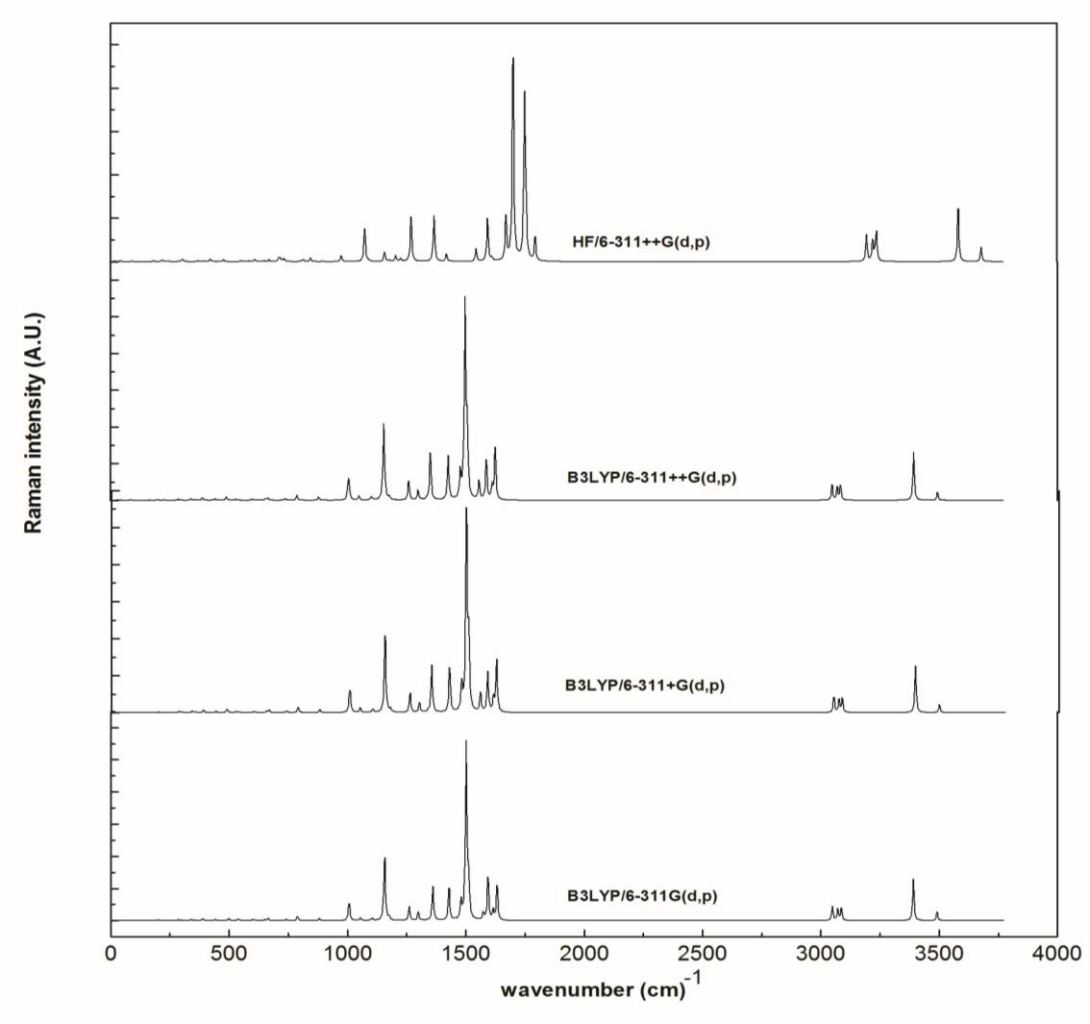

Figure 6. Calculated Raman spectra of AMNT at various level of theory

Calculated phenyl ring vibrations are in good agreement with the experimental data [11]. The selection rule for meta-substituted phenyl ring allows four C–H stretching vibrations. Although the DFT predict all these four bands, but these are observed as inseparable in IR. Usually Raman has one strong band in this zone [36]. The ring CH stretching vibrations appear to be very weak, which is due to steric interaction that induces effective conjugation and charge carrier localization resulting in twisted phenyl ring [37]. The carbon hydrogen stretching vibrations give rise to bands in the region 3100–3000 cm^{-1} in all the aromatic compounds [38]. The C–H stretching vibrations of phenyl ring are calculated at 3084, 3070 and 3048 cm^{-1} in AMNT but in CDMABA[39], these bands are found at 3045, 3061 cm^{-1} in IR spectra and at 3057, 3069 cm^{-1} in Raman spectra respectively while in AMNO[35] these modes are observed at 3080 cm^{-1} . Minor shift may arise due to the influence of nitro group attached to the phenyl ring in title compound. There are six vibrational modes of C-C stretching with a contribution of ring bending, which are more substituent dependent, calculated corresponding to the peaks at 1003, 1097, 1335, 1426, 1587 and 1625 cm^{-1} with other mode of vibrations [39]but in AMNO[35] these are reported at 1569 and 1480 cm^{-1}, shown in PED table-3. These modes of phenyl ring are also having contributions in the vibrations of substituent nitro group and thiadiazole ring. The in-plane CH bending vibrational modes of the phenyl ring, are found as a series of bands at 1178, 1299, 1316, 1426 and1478 cm^{-1} in the range 1003-1626 cm^{-1}. PED assignment shows that these vibrations have coupling with C-C stretching of the ring and the other vibrational modes of substituents. The CH out-of-plane bending modes of the phenyl ring vibrations corresponding to medium, strong and weak bands are calculated at 813, 913, 953 and 1007 cm^{-1}, having contribution in other modes are shown in Table 3 and are assigned to ring in-plane deformation modes. The puckering modes of phenyl ring (ring-2) with a contribution of out-of-plane bending of the substituents are calculated at 674 cm^{-1}. Other fundamental modes of phenyl ring that show similar characteristics like torsional modes and their assignments have also been calculated and shown in table 3 with their corresponding potential energy distributions.

Table 3. Potential Energy Distribution and vibrational wavenumbers of AMNT

Unscaled				Scaled				Calculated		Obserbed Ir	Assignments B3LYP/6-311++G(d,p)
B3LYP/ 6-311++ G (d,p)	B3LYP/ 6-311+G (d,p)	B3LYP/ 6-311G (d,p)	HF/ 6-311++G (d,p)	B3LYP/ 6-311++G (d,p)	B3LYP/ 6-311+G (d,p)	B3LYP/ 6-311G (d,p)	HF/ 6-311++G (d,p)	Ir	Raman activity		
3683.52	3684.1	3680.28	3892.82	3494.403	3494.918	3491.524	3679.677	47.27	0.036847	3225	(N1H16)(61)+ $_{as}$(N1H17)(34)+ (NH_2)(6)
3570.28	3570.63	3567.58	3782.99	3393.567	3393.879	3391.158	3582.632	98.32	0.035896	3050	(N1H17)(62)+ (N1H16)(32)+ (NH_2)(5)
3226.25	3226.55	3228.92	3395.99	3084.657	3084.928	3087.069	3237.551	4.74	0.029455		(C10H21)(96)+ (C11H19)(3)
3211.05	3211.37	3212.46	3389.15	3070.919	3071.209	3072.194	3231.408	3.08	0.010778		(C12H18)(89)+ (C11H19)(7)
3210.67	3210.61	3211.71	3378	3070.576	3070.522	3071.516	3221.391	5.95	0.010695		(C8H20)(97)
3186.69	3187.06	3186.76	3349.09	3048.888	3049.223	3048.951	3195.4	6.51	0.003647		(C11H19)(89)+ $_{as}$ (C12H18)(8)
1655.73	1655.72	1662.74	1833.28	1625.449	1625.44	1632.141	1794.447	23.33	2.37631		(C8C9)(19)+ (C11C12)(15)+ $_{as}$(C9C10)(11)+ $_{as}$(NO_2)(8)+ $_{asym}$ (ring2)(8)+ $_{as}$(C7C12)(6)+ (N13O14)(6)+ (N13O15)(5)+ (C8C10-N13-C9)(5)+ (C11C7-H18-C12)(5)+ (C7C9-H20-C8)(3)+ (C10C12-H19-C11)(3)
1641.9	1641.95	1645.45	1793.01	1612.242	1612.29	1615.633	1756.207	210.44	5.383873		(NH_2)(81)+ (N1C2)(13)
1616.39	1616.45	1622.46	1786.9	1587.865	1587.923	1593.668	1750.4	46.14	3.323527		(C7C8)(20)+ (C10C11)(17)+ $_{as}$(C9C10)(13)+ $'_{asym}$(ring2)(8)+ (C9C11-H21-C10)(7)+ (C7C9-H20-C8)(6)+ (N13O15)(5)+ (C7C12)(5)+ (NO_2)(3)
1584.24	1584.34	1601.77	1758.89	1557.113	1557.209	1573.885	1723.765	233.63	1.400663		(N13O14)(33)+ $_{as}$(N13O15)(32)+ (NO_2)(14)+ $_{as}$(C7C12)(5)+ (C11C7-H18-C12)(3)
1532.19	1532.24	1537.36	1735.15	1507.254	1507.302	1512.21	1701.171	75.71	6.395193	1619	(N5C6)(23)+ $_{as}$(N4C2)(18)+ $_{as}$(C6C7)(15)+ (N1C2)(8)+ (NH_2)(6)+ (C10C12-H19-C11)(5)+ $_{as}$(C10C11)(5)+ (C11C7-H18-C12)(4)
1522.48	1522.55	1526.36	1703.76	1497.943	1498.01	1501.664	1671.267	330.27	5.536661	1517	(N4C2)(29)+ $_{as}$(N1C2)(17)+ (N5C6)(15)+ (NH_2)(11)+ $_{as}$(C6C7)(6)+ (ring1)(6)
1501.7	1501.78	1503.98	1641.26	1478.007	1478.083	1480.195	1611.631	15.31	0.974939		(C10C12-H19-C11)(22)+ $_{as}$(N5C6)(22)+ (C7C9-H20-C8)(12)+ (C7C12)(7)+ $_{as}$(C9C10)(7)+ (C9C11-H21-C10)(5)+ (C11C12)(4)+ (C11C7-H18-C12)(4)+ $_{as}$(C10C11)(3)+ $_{as}$(C8C9)(3)
1448.44	1448.47	1451	1622.28	1426.844	1426.873	1429.306	1593.496	8.48	0.626701		(C8C9)(21)+ $_{as}$(N5C6)(14)+ (C11C7-H18-C12)(14)+ $_{as}$(C11C12)(13)+ (C9C11-H21-C10)(12)+ (C7C8)(5)+ (C8C10-N13-C9)(4)+ $_{as}$(C9C10)(3)
1370.16	1370.33	1380.16	1571.54	1351.48	1351.644	1361.118	1544.956	332.97	0.971541		(N13O14)(37)+ (N13O15)(36)+ $_{as}$(C9N13)(20)+ (NO_2)(4)
1353.8	1353.87	1354.58	1459.97	1335.704	1335.771	1336.456	1437.928	7.65	0.484253		(C7C8)(18)+ $_{as}$(C7C12)(15)+ $_{as}$(C10C11)(14)+ (C11C12)(13)+ (C9C10)(11)+ (C9C11-H21-C10)(8)+ $_{as}$(C8C9)(7)+ (C7C9-H20-C8)(4)+ (C11C7-H18-C12)(3)
1334.1	1334.09	1336.49	1441.06	1316.696	1316.686	1319.002	1419.748	49.12	2.910708	1556	(NH_2)(21)+ (N1C2)(18)+ $_{as}$(S3C2)(10)+ (N4C2)(10)+ $_{asym}$(S3N4N1C2)(7)+ (ring1)(6)+ (C11C7-H18-C12)(4)+ (NH_2)(3)
1316.38	1316.38	1315.95	1386.65	1299.587	1299.587	1299.172	1367.372	16.97	0.365284		(C7C9-H20-C8)(17)+ (C10C12-H19-C11)(14)+ (C11C7-H18-C1

										2)(10)+ $_{as}$(C7C12)(10)+ (NH_2)(5)+ (C7C8)(5)+ (C9C11-H21-C10)(4)+ $_{asym}$'(C12C8C6C7)(4)+ (C6C7)(4)+ $_{as}$(C8C9)(4)+ $_{as}$(C9C10)(4)+ $_{as}$(N4C2)(3)
1275.41	1275.45	1276.71	1331.04	1259.991	1260.03	1261.249	1313.742	32.61	0.414056		(C6C7)(24)+ . C7C9-H20-C8)(17)+ (N5C6)(11)+ $_{tri}$(ring2)(9) + $_{as}$(N4N5)(7)+ '(ring1)(6)+ $_{as}$(S3C6)(4)
1191.11	1191.16	1189.86	1286.06	1178.347	1178.396	1177.135	1270.289	1.31	2.324152		(C10C12-H19-C11)(37)+ (C11C7-H18-C12)(27)+ (C9C11-H21-C10)(15)+ $_{as}$(C11C12)(11)+ (C10C11)(6)
1166.7	1166.73	1169.3	1240.5	1154.663	1154.692	1157.187	1226.209	36.78	2.131877	995	(N4N5)(49)+ $_{as}$(N4C2)(17)+ '(ring1)(9)+ (NH_2)(7)+ $_{as}$(N1C2)(7)
1114.27	1114.26	1115.55	1218.72	1103.726	1103.716	1104.971	1205.113	51.6	0.345209		(C9N13)(25)+ (C7C9-H20-C8)(17)+ $_{as}$(C9C10)(16)+ $_{as}$(C8C9)(14)+ (C9C11-H21-C10)(10)+ $_{tri}$(ring2)(5)+ (NO_2)(3)
1108.38	1108.39	1107.85	1190.84	1097.998	1098.008	1097.483	1178.085	3.83	0.186767		(C10C11)(28)+ (C9C11-H21-C10)(22)+ (C11C7-H18-C12)(17)+ (C11C12)(12)+ $_{as}$(C7C8)(5)+ (C7C9-H20-C8)(3)
1058.82	1058.69	1063.52	1170.17	1049.758	1049.631	1054.336	1158.031	32.07	0.345642		(NH_2)(41)+ $_{as}$(N4N5)(26)+ $_{as}$(N4C2)(13)+ (ring1)(8)+ $_{as}$(N1C2)(3)
1015.54	1016.33	1017.13	1124.75	1007.565	1008.335	1009.116	1113.915	5.69	2.319755		$_{tri}$(ring2)(66)+ '(ring1)(7)+ (C9C10)(6)+ (C8C9)(5)+ (C9N13)(3)
1015.32	1015.4	1015.83	1101.66	1007.35	1007.428	1007.848	1091.462	0.25	2.072082		ω(H19C10C12C11)(41)+ω(H18C11C7C12)(35)+ω(H21C9C11C10)(10)+Puck(ring2)(9)+τ'$_{asym}$(ring2)(4)
1011.53	1011.48	1011.87	1084.03	1003.652	1003.603	1003.984	1074.307	13.92	1.019461		(C7C12)(25)+ '(ring1)(24)+ (C7C8)(10)+ (C11C12)(9)+ $_{as}$(S3C6)(8)+ $_{as}$(C9N13)(4)
960.09	960.61	964.95	1076.14	953.4179	953.9261	958.1677	1066.626	0.06	0.039213		ω(H21C9C11C10)(52)+ω(H18C11C7C12)(32)+τ$_{asym}$(ring2)(6)+ω(H19C10C12C11)(4)
918.79	915.57	923.78	1028.1	913.0234	909.8717	917.907	1019.816	12.21	0.036854		ω(H20C7C9C8)(74)+Puck(ring2)(13)+ω(C6C12C8C7)(4)
884.21	884.29	886.34	982.4	879.1588	879.2372	881.2459	975.2156	28.01	0.441298		(NO_2)(29)+ (C9N13)(23)+ '(ring1)(9)+ $_{tri}$(ring2)(6)+ (N13O15)(5)+ (N13O14)(4)+ (C8C9)(4)+ '$_{asym}$(ring2)(3)+ (C9C10)(3)+ $_{asym}$(ring2)(3)
817.49	817.74	825.61	902.19	813.709	813.9545	821.6822	896.7717	31.71	0.06229		ω(H19C10C12C11)(31)+ω(H21C9C11C10)(27)+ω(H18C11C7C12)(18)+Puck(ring2)(11)+ω(N13C8C10C9)(5)+ω(C6C12C8C7)(4)+ω(NO_2)(3)
790.93	790.96	792.63	849.85	787.6143	787.6438	789.2852	845.4711	3.55	0.850407		'(ring1)(27)+ (ring1)(19)+ (NO_2)(14)+ $_{as}$(S3C6)(10)+ $_{as}$(N1C2)(7)+ $_{asym}$(ring2)(7)+ (C6C7)(5)
742.38	742.42	743.11	819.53	739.8553	739.8947	740.574	815.7124	56.67	0.337756		(NO_2)(36)+ (S3C6)(18)+ $_{asym}$(ring2)(12)+ '$_{asym}$(ring2)(8)+ (C9N13)(6)+ '$_{asym}$(C12C8C6C7)(5)+ (S3N5-C7-C6)(3)
731.65	732.29	742.96	812.86	729.2898	729.9201	740.4263	809.1618	8.92	0.142847		ω(NO_2)(60)+ω(C6C12C8C7)(11)+ω(N13C8C10C9)(9)+Puck(ring2)(7)+ω(H21C9C11C10)(4)
675.95	669.72	687.71	736.63	674.3832	668.2356	685.9841	734.1939	27.21	0.198823		Puck(ring2)(63)+ω(C6C12C8C7)(14)+ω(H19C10C12C11)(10)+ω(N13C8C10C9)(7)+ω(NO_2)(3)
666.95	666.93	667.13	728.95	665.5019	665.4821	665.6795	726.6306	8.15	0.677351		'$_{asym}$(ring2)(41)+ $_{asym}$(ring2)(10)+ $_{as}$(S3C2)(10)+ (NO_2)(8)+ $_{as}$(S3C6)(6)+ (S3N5-C7-C6)(4)+ $_{as}$(C9N13)(3)
654.69	654.58	651.17	720.57	653.3993	653.2907	649.9236	718.3757	6.99	0.418988	912	(S3C2)(60)+ $_{asym}$(S3N4N1C2)(10)+ '$_{asym}$(ring2)(6)+ (NH_2)(4)+ (N1C2)(3)+- '(ring1)(3)

623	623.01	631.16	713.18	622.0936	622.1035	630.1578	711.0941	41.38	0.08763		ω(N1S3N4C2)(35)+τ'(ring1)(26)+ω(N1H16H17C2)(17)+ (NH_2)(12)
609.25	608.26	610.23	671.09	608.5002	607.5212	609.4692	669.5876	2.1	0.146159		τ(ring1)(44)+ω(C7S3N5C6)(27)+Puck(ring2)(11)+ω(C6C12C8C7)(5)+ω(N13C8C10C9)(3)+τ_{asym}(ring2)(3)
599.43	599.49	599.39	651.03	598.7882	598.8475	598.7486	649.7854	0.07	0.340487		(ring1)(31)+ $_{asym}$(ring2)(17)+ (S3C6)(8)+ω(N1S3N4C2)(7)+τ'(ring1)(7)+ '(ring1)(5)+ (S3N5-C7-C6)(5)+ (NO_2)(4)+ $_{as}$(N1C2)(4)+ '$_{asym}$(C12C8C6C7)(3)
541.96	541.92	544.98	609.31	541.8874	541.8478	544.8802	608.5595	8.51	0.138919		(NO_2)(40)+ (C8C10-N13-C9)(15)+ω(N1H16H17C2)(10)+ (ring1)(5)+ (NH_2)(5)+ (S3C6)(4)+ $_{as}$(C9C10)(4)+ $_{asym}$(ring2)(3)
528.55	527.41	537.22	586.47	528.5947	527.4644	537.1895	585.966	64.09	0.418472		ω(N1H16H17C2)(27)+ (NH_2)(19)+τ_{asym}(ring2)(14)+τ(ring1)(9)+ω(C6C12C8C7)(8)+ω(N13C8C10C9)(7)+Puck(ring2)(5)
489.62	487.8	498.41	551.32	489.9721	488.1653	498.697	551.162	211.04	1.024754		ω(N1H16H17C2)(47)+ (NH_2)(32)+τ_{asym}(ring2)(5)
439.88	439.92	440.52	476.73	440.553	440.5928	441.1894	477.173	5.55	0.42052		(S3N5-C7-C6)(15)+ $_{asym}$(S3N4N1C2)(14)+ (NO_2)(9)+ (S3C6)(9)+ (C9N13)(9)+ '$_{asym}$(C12C8C6C7)(8)+ '$_{asym}$(ring2)(8)+ (NO_2)(7)+ (ring1)(6)+ $_{asym}$(ring2)(5)
424.75	425.34	431.03	460.74	425.5046	426.0916	431.7516	461.2883	2.15	0.058282		τ'$_{asym}$(ring2)(64)+ω(N13C8C10C9)(22)+ω(H18C11C7C12)(4)
387.49	387.55	388.05	421.06	388.4137	388.4735	388.9715	421.8334	0.65	0.684071		$_{asym}$(S3N4N1C2)(28)+ (NO_2)(20)+ (C9N13)(19)+ '$_{asym}$(ring2)(9)+ $_{asym}$(ring2)(5)
354.74	354.74	354.57	395.23	355.775	355.775	355.6055	396.1223	22.82	0.169974		τ_{asym}(ring2)(28)+ω(C7S3N5C6)(18)+ω(N1H16H17C2)(15)+ (NH_2)(9)+τ'(ring1)(8)+ω(N1S3N4C2)(7)+τ(N1C2)(5)
338.67	338.73	339.1	368.67	339.7469	339.8067	340.1759	369.662	0.45	0.399015		$_{asym}$(S3N4N1C2)(26)+ '$_{asym}$(C12C8C6C7)(17)+ (C8C10-N13-C9)(10)+ (S3C6)(10)+ (NO_2)(9)+ (NO_2)(4)+ $_{as}$(C9N13)(4)+τ(N1C2)(3)
295.91	295.65	297.41	304.36	297.0571	296.7974	298.5557	305.498	38.32	0.130658		τ(N1C2)(42)+ω(N1H16H17C2)(24)+ (NH_2)(16)+ω(N1S3N4C2)(9)
283.86	283.86	284.32	298.63	285.0162	285.0162	285.4759	299.7744	0.51	0.303025		(C6C7)(23)+ $_{asym}$(ring2)(15)+ '(ring1)(12)+ (S3C6)(8)+τ(N1C2)(5)+ (C9N13)(4)+ (NO_2)(4)+ $_{tri}$(ring2)(4)+ (ring1)(3)
224.31	224.34	225.42	244.5	225.4414	225.4714	226.5529	245.6527	3.72	0.095673		(C8C10-N13-C9)(42)+ (S3N5-C7-C6)(22)+ (NO_2)(8)+ $_{asym}$(S3N4N1C2)(7)+ (C7C8)(5)+ $_{as}$(S3C6)(4)
197.59	197.97	198.86	217.94	198.6727	199.0535	199.9455	219.0619	1.21	0.185573		τ_{asym}(ring2)(41)+τ'(ring1)(18)+τ(ring1)(6)+ω(H18C11C7C12)(5)+ω(C6C12C8C7)(5)+τ'$_{asym}$(ring2)(5)+ω(N13C8C10C9)(4)+ω(N1S3N4C2)(4)+ω(H21C9C11C10)(4)
162.41	162.34	164.96	180.62	163.393	163.3228	165.9516	181.6596	3.86	0.064196		ω(N13C8C10C9)(35)+τ'$_{asym}$(ring2)(20)+τ'(ring1)(10)+ω(H20C7C9C8)(9)+ω(NO_2)(6)+ω(H21C9C11C10)(4)+τ(ring1)(3)+Puck(ring2)(3)
85.3	85.32	85.9	93.18	85.92351	85.94363	86.52706	93.84914	4.94	0.103695		'$_{asym}$(C12C8C6C7)(42)+ρ(S3N5-C7-C6)(34)+ ρ(C8C10-N13-C9)(11)
79.82	79.75	81.82	86.25	80.41058	80.34016	82.42271	86.87912	2.09	0.069072		ω(C7S3N5C6)(41)+ω(C6C12C8C7)(23)+τ(C9-N13)(12)+τ'(ring1)(9)+ω(H20C7C9C8)(3)
42.2	41.61	46.58	41.25	42.53811	41.94379	46.94988	41.58114	0.13	0.052061		τ(C9-N13)(79)+τ_{asym}(ring2)(11)
27.31	27.01	29.1	15.57	27.53544	27.2331	29.33937	15.70151	6.23	0.076976		τ(C6C7)(86)+ω(C6C12C8C7)(3)

Types of vibration: stretching(ν), deformation (bending) (δ), scissoring (λ), wagging(ω), rocking(ρ), torsion (τ), Puckering(Puck).

Nitro group compounds show a very strong asymmetric stretch at 1540–1614 cm^{-1} and a strong symmetric stretch at 1320–1390 cm^{-1} [40]. For this title compound a very strong band corresponding to asymmetric stretch at 1557 cm^{-1} and a strong band at 1351 cm^{-1} corresponding to symmetric stretch are calculated by DFT and reported at 1550 and 1350 cm^{-1} for AMNO[35]. According to Peticolas and co-workers it has been found that the NO_2 symmetric stretching vibration occurs at 1364 cm^{-1} in a series of chemically related p-nitro substituted derivatives [41]. NO_2 group scissoring modes are assigned at frequencies 739 and 879 cm^{-1}. Rocking modes of NO_2 are found at 541 cm^{-1} and out of plane bending of NO_2 group calculated at 729 cm^{-1}.

The N–H group attached to the hetero aromatic molecule shows stretching mode in the usual range 3500–3220 cm^{-1} of appearance for NH_2, CH_3 and C–H stretching vibrations. These absorptions depend upon the degree of hydrogen bonding and the physical state of the sample or the polarity of the solvent [42]. The N–H stretching vibrational bands are sharper and weaker than O–H stretching vibrations by virtue of which they can be easily identified [43]. The N–H stretching fundamental of piperidine was observed in the vapor phase at 3364cm^{-1} [44] and in the liquid phase at 3340cm^{-1} for the N–H stretching of the piperidine [34, 45]. For our compound the stretching vibrations of the amino group associated with thiadiazole ring are experimentally observed in the range 3050–3225 cm^{-1} [11], which are calculated at 3393 and 3494 cm^{-1} conforms the NH stretching vibrations. The out-of-plane bending of amino group are calculated at 489 and 528 cm^{-1} mixed with other modes of vibrations of ring-1, which are shown in Potential energy distribution table.

4. Conclusions

Geometry of AMNT molecule was optimized using DFT at various levels of theory and also HF employing 6-311++G(d,p) basis set. The calculated values are also compared with experimental data. In general the structural parameters matches well with the experimental one, with few exceptions caused due to constraints imposed by isolated molecule model. Potential energy scan suggested one less stable conformer in which two rings are almost twisted by 180^o. A detailed normal coordinate analysis of all the normal modes along with PED very clearly indicates the composition of each normal mode in terms of internal coordinates. Predictive IR and Raman spectra are very useful in the absence of experimental data. HOMO-LUMO, EPS and NBO may serve as a useful quantity to explain hydrogen bonding, reactivity and structure–activity relationship of molecules.

ACKNOWLEDGEMENTS

Financial assistance to Mahesh Pal Singh Yadav from Jaypee University of Engg. & Technology, Guna is gratefully acknowledged.

REFERENCES

[1] Geeta Mishra, Arvind K. Singh and Kshtiz Jyoti, 2011, Review article on 1, 3, 4-Thiadiazole derivaties and it's Pharmacological activities., International Journal of Chem Tech Research, 3(3), 1380-1393.

[2] G.L. Almajan, A. Innocenti, L. Puccetti, G. Manole, S. Barbuceanu, I. Saramet, A. Scozzafava, and C.T. Supuran, Carbonic anhydrase inhibitors. Inhibition of the cytosolic and tumor-associated carbonic anhydrase isozymes I, II, and IX with a series of 1,3,4-thiadiazole- and 1,2,4-triazole -thiols., Bioorg. Med. Chem. Lett., vol. 15 pp. 2347-2352, 2005.

[3] J.Y. Chou, S.Y. Lai, S.L. Pan, G.M. Jow, J.W. Chern, and J.H. Guh, 2003, Investigation of anticancer mechanism of thiadiazole-based compound in human nonsmall cell lung cancer A549 cells, Biochem. Pharmacol., 66(1), 115-124.

[4] F. Clerici, D. Pocar, M. Guido, A. Loche, V. Perlini and M. Brufani, 2001, Synthesis of 2-amino-5-sulfanyl-1,3,4-thiadiazole derivatives and evaluation of theirantidepressant and anxiolytic activity, J. Med. Chem., 44(6), 931-936.

[5] N. Demirbas, S.A. Karaoglu, A. Demirbas and K. Sancak, 2004, Synthesis and antimicrobial activities of some new 1-(5-phenylamino-[1,3,4]thiadiazol-2-yl) methyl-5-oxo- [1,2, 4] triazole and 1-(4-phenyl-5-thioxo -[1,2,4] triazol-3-yl) methyl-5-oxo -[1,2,4]triazole derivatives, Eur. J. Med. Chem., 39(9), 793-804.

[6] K. Desai and A.J. Baxi, 1992, Studies on 2-azetidinone: Part VI Synthesis and antimicrobial activity of 5-(2',4'-dichlorophenoxymethyl)-2-(4"-aryl-3"-chloro-2"-az etidinone-1"-yl)-1,3,4-thiadiazole, Indian J. Pharm. Sci., 54(5), 183-188.

[7] J. Sandstrom, 1968, Recent Advances in the Chemistry of 1,3,4-Thiadiazoles, Adv. Heterocycl. Chem., 9, 165-209.

[8] Arvind k. singh, R.Parthsarthy, Kshitiz jyoti and Geeta mishra, 2011, Synthesis, characterization and antibacterial activity of 1, 3, 4-thiadiazole derivatives, IJSID, 1(3), 353-361.

[9] F. A. Adam, 1987, Zinc(II), Cobalt(II) and Nickel(II) Complexes of 5-Substituted-1,3,4-Thiadiazoles, J. Chin. Chem. Soc. (Taipei, Taiwan)**,** 34(2), 111-115.

[10] Thoraya A. Farghaly, Magda A. Abdallah and Mohamed R. Abdel Aziz, 2012, Synthesis and Antimicrobial Activity of Some New 1,3,4-Thiadiazole Derivatives, Molecules, 17, 14625-14636.

[11] M. M. Ishankhodzhaeva, M. D. Surazhskaya, A. E. Mukhammedov, and P. A. Koz'min, 2006, Crystal and Molecular Structures of 2-Amino-5-(m-Nitrophenyl)-1, 3, 4-Thiadiazole, Crystallography Reports, 51(1), 68-71.

[12] P. Hohenberg and W. Kohn, 1964, Inhomogeneous Electron Gas, Phys. Rev. vol. 136, B864-B871.

[13] M.J. Frisch, G.W. Trucks, H.B. Schlegel, G.E. Scuseria, J.R. Cheeseman, M.A. Robb, G. Scalmani, V. Barone, B.

Mennucci, G.A. Petersson, H. Nakatsuji, M. Caricato, X. Li, H.P. Hratchian, A.F. Izmzylov, J. Bloino, G. Zheng, J.L. Sonnenberg, M. Hada, M. Ehara, K. Toyota, R. Fukuda, J. Ishida, M. Hasegawa, T. Nakajima, Y. Honda, O. Kitao, H. Nakai, T. Vreven, J.A. Montgomery Jr., J.E. Peralta, F. Ogliaro, M. Bearpark, J.J. Heyd, E. Brothers, K.N. Kudin, V.N. Staroverov, R. Kobayashi, J. Normand, A. Raghavachari, A. Rendell, J.C. Burant, S.S. Iyengar, J. Tomasi, M. Cossi, N. Rega, J.M. Millan, M. Klene, J.E. Knox, J.B. Cross, V. Bakken, C. Adamo, J. Jaramillo, R. Gomperts, R.E. Stratmann, O. Yazyev, A.J. Austin, R. Cammi, C. Pomelli, J.W. Ochterski, R.L. Martin, K. Morokuma, V.G. Zakrzewski, G.A. Voth, P. Salvador, J.J. Dannerberg, S. Dapprich, A.D. Daniels, J. Farkas, B. Foresman, J.V. Ortiz and J. Cioslowski, D.J. Fox, Gaussian 09; Revision B.01, Gaussian, Inc., Wallingford CT, 2010.

[14] C.T. Lee, W.T. Yang and R.G. Parr, 1988, Development of the Colle-Salvetti correlation-energy formula into a functional of the electron density, Phys. Rev. B, vol. 37 No. 2, 785-789.

[15] R.G. Parr and W. Yang, 1989, Density Functional Theory of Atoms and Molecules, Oxford University Press, New York.

[16] A.D. Becke, 1993, Density-functional thermochemistry. III. The role of exact exchange, J. Chem. Phys. 98, 5648-5652.

[17] F. Weinhold and C.R. Landis, 2001, Natural bond orbitals and extensions of localized bonding concepts, Chem. Educ. Res. Pract. Eur., 2, 91–104.

[18] C. James, G.R. Pettit, O.F. Nielsen, V.S. Jayakumar and I. Hubert Joe., 2008, Vibrational spectra and ab initio molecular orbital calculations of the novel anti-cancer drug combretastatin A-4 prodrug, Spectrochimica Acta Part A, 70(5), 1208–1216.

[19] P. Pulay, G. Fogarasi, F. Pang and J.E. Boggs, 1979, Systematic ab initio gradient calculation of molecular geometries, force constants, and dipole moment derivatives, J. Am. Chem. Soc., 101(10), 2550-2560.

[20] G. Fogarasi, X. Zhou, P.W. Taylor and P. Pulay, 1992, The calculation of ab initio molecular geometries: efficient optimization by natural internal coordinates and empirical correction by offset forces, J. Am. Chem. Soc., 114(21), 8191-8201.

[21] J.M.L Martin and C. Van Alsenoy, Gar2ped, University of Antwerp, 1995.

[22] H. Yoshida, K. Takeda, J. Okamura, A. Ehara and H. Matsurra, 2002, A New Approach to Vibrational Analysis of Large Molecules by Density Functional Theory: Wavenumber-Linear Scaling Method, J. Phys. Chem. A, 106(14), 3580-3586.

[23] A.E. Reed, L.A. Curtiss and F. Weinhold, 1988, Intermolecular interactions from a natural bond orbital, donor-acceptor viewpoint, Chem. Rev., 88(6), 899-926.

[24] J. Chocholousova, V. Vladimir Spirko and P. Hobza, 2004, First local minimum of the formic acid dimer exhibits simultaneously red-shifted O–H ▪▪▪ O and improper blue-shifted C–H▪▪▪O hydrogen bonds, Phys. Chem. Chem. Phys., 6, 37-41.

[25] F. H. Allen, 1984, The geometry of small rings. VI. Geometry and bonding in cyclobutane and cyclobutene, Acta Crystallogr.B, 40, 64-72.

[26] C. Yuksektepe, N. Calıskan, I. Yılmaz and A. Cukurovali, 2006, 2-{[4-(3-Mesityl-3-methylcyclobutyl) thiazol-2-yl] hydrazono}-1,2-diphenylethanol ethanol solvate, Acta Crystallogr. E, 62(7), 2762-2764.

[27] F. Weinhold and C.R. Landis, 2005, "Valency and bonding: A Natural Bond Orbital Donor- Acceptor Perspective", Cambridge University Press, UK.

[28] P. Politzer and D.G. Truhlar (Eds.), 1981 "Chemical Applications of Atomic and Molecular Electrostatic Potentials", Plenum Press, New York.

[29] S. Gunsekaran, R.A. Balaji, S. Kumeresan, G. Anand and S. Srinivasan, 2008, Can. J. Anal. Sci. Spectrosc., 53, 149-160.

[30] R.G. Pearson, 1989, Absolute electronegativity and hardness: applications to organic chemistry, J. Org. Chem., 54(6), 1423–1430.

[31] P. Geerlings, F.D. Proft and W. Langenaeker, 2003, Conceptual Density Functional Theory, Chem. Rev., 103, 1793–1873.

[32] R.G. Parr, L.V. Szentpaly and S. Liu, 1999, Electrophilicity Index, J. Am. Chem. Soc., 121(9), 1922–1924.

[33] P.K. Chattaraj and S. Giri, 2007, Stability, Reactivity, and Aromaticity of Compounds of a Multivalent Superatom, J. Phys. Chem. A, 111(43), 11116–11121.

[34] J. Padmanabhan, R. Parthasarathi, V. Subramaniaan and P.K. Chattaraj, 2007, Electrophilicity-Based Charge Transfer Descriptor, J. Phys. Chem. A, 111(7), 1358–1361.

[35] Ibtisam, 2011, Synthesis, characterization and investigation of biological activity ofnew heterocyclic compounds, K. Jassim; K. J. Pharm . Sci, 2, 196-217.

[36] F.R. Dollish, W.G. Fateley and F.F. Bentley, 1974, Characteristic Raman Frequencies of Organic Compounds, Wiley, New York.

[37] H. Neugebauer, C. Kvarnstrom, C. Brabec, N.S. Sariciftci, R. Kiebooms, F. Wudl and S. Luzzati, 1999, Infrared spectroelectrochemical investigations on the doping of soluble poly(isothianaphthene methine) (PIM), J. Chem. Phys., 110(12), 12108-12115.

[38] B. Smith, 1999, Infrared Spectral Interpretation. A Systematic Approach, CRC Press, Washington, DC.

[39] Sapna Pathak, Anuj Kumar and Poonam Tandon, 2010, Molecular structure and vibrational spectroscopic investigation of 4-chloro-4'dimethylamino-benzylidene aniline using density functional theory, J. Mol. Struct, 98(1-3), 1-9.

[40] E.K. Meislich, H. Meislich and J. Sharefkin, 1993, 3000 Solved Problems in Organic Chemistry, vol. 2, McGraw-Hill, New York.

[41] E.D. Schmid, M. Moschallski and W.L. Peticolas, 1986, Solvent effects on the absorption and Raman spectra of aromatic nitrocompounds. Part 1. Calculation of preresonance Raman intensities, J. Phys. Chem., 90(11), 2340-2346.

[42] S. Gunasekaran, S.R. Varadhan and K. Manoharan, 1993, Asian J. Phys., 2, 165-172.

[43] S. Gunasekaran, R.K. Natarajan, R. Rathikha and D. Syamala, 2005, Vibrational spectra and normal coordinate analysis of nalidixic acid, Ind. J. Pure Appl. Phys.,43, 503-508.

[44] D. Vedal, O. Ellestad and P. Klaboe, 1976, The vibrational spectra of piperidine and morpholine and their N-deuterated analogs, Spectrochim. Acta A, 32(4), 877-890.

[45] M.T. Gulluoglu and S. Yurdakul, 2001, Infrared spectroscopic studies of some piperidine metal(II) clathrates: $M(C_5H_{11}N)_2Ni(CN)_4 G$ (M = Co, Ni; G = m-xylene, p-xylene or o-xylene; M = Ni; G = dioxane), Vib. Spectrosc., 25(2), 205-211.